UNIVERSITY OF CALIFORNIA, SAN DIEGO

Adaptive Design & Optimization of 3D Printable, Shape-Changing, Ballistically Deployable Drone Platforms

A thesis submitted in partial satisfaction of the
requirements for the degree
Master of Science

in

Structural Engineering

by

Luke Henderson

Committee in charge:

Professor Falko Kuester, Chair
Professor Thomas Bewley
Professor John B. Kosmatka

2017

The thesis of Luke Henderson is approved, and it is acceptable in quality and form for publication on microfilm and electronically:

_____

_____

_____

Chair

University of California, San Diego

2017

EPIGRAPH

Design is not just what it looks like and feels like. Design is how it works.

—Steve Jobs

TABLE OF CONTENTS

LIST OF FIGURES

ACKNOWLEDGEMENTS

Thanks to Twain Glaser for his participation in the development of the GLAD platform from concept to fully fledged prototype.

Thanks to my parents for their support and for letting me borrow their car with the optimistic hope of someday seeing it returned.

Thanks to the members of CISA3 and DroneLab for their assistance in work and in procrastination.

Thanks also to Erwin Ho for showing me the ins and outs of San Diego and helping me make the best of my time here.

And finally, thanks to the coffee cart outside Atkinson hall as well as ”BirdRock Coffee Roaster’s” who’s chocolate chip cookies and coffee, respectively, helped fuel this work.

Chapter 2, in great part, is a reprint of the material as it appears in “Towards Bio-Inspired Structural Design of a 3D Printable, Ballistically Deployable, Multi-Rotor UAV”, *IEEE Aerospace Conference*, 2017. Luke W. Henderson, Twain Glaser, Falko Kuester. The thesis author was the primary author of this paper.

VITA

2015	B. S. in Civil Engineering, Columbia University, New York
2017	Ms. in Structural Engineering, University of California, San Diego

PUBLICATIONS

Luke W. Henderson, Twain Glaser, Falko Kuester, "Towards Bio-Inspired Structural Design of a 3D Printable, Ballistically Deployable, Multi-Rotor UAV", *IEEE Aerospace Conference*, 2017.

ABSTRACT OF THE THESIS

Adaptive Design & Optimization of 3D Printable, Shape-Changing, Ballistically Deployable Drone Platforms

by

Luke Henderson

Master of Science in Structural Engineering

University of California, San Diego, 2017

Professor Falko Kuester, Chair

This thesis will present an alternative UAV design to address issues encountered by conventional platforms when deploying in under harsh conditions. The design proposed is a ballistically deployed UAV platform, or Ground-Launched, Air-Deployable (GLAD) platform to be either projectile launched from the ground or inserted into the target environment from above via a 'parent' aircraft. This gives it the ability to punch through sparse ground cover or be tossed clear of hazardous ground conditions such as turbulent winds, before deploying above. Furthermore, this thesis will look into new design strategies applied to the conception of such a platform: when designing a UAV with

the very broad goal of facilitating deployment in field conditions, the widely differing operating environments which this infers are so broad as to make an ideal design for this job a superfluous notion: jack of all trades, master of none. Because of this, and the empowerment brought on by 3D printing, this thesis suggests a new, more efficient design process for small ballistic 3D printed UAV platforms.

By creating a work-flow which allows for the individual optimization and design of each aspect of the platform's design, a single process can be used to design multiple platforms with varying designs for various applications in various environments. Thus doing away with the age-old engineering tradition of creating one-size-fits-all designs.

Chapter 1

Introduction

Multi-rotor unmanned aerial vehicles (UAVs) are widely popular among hobbyists and professionals and have evolved from toys into fully featured imaging platforms. These are sensor platforms that are readily being used for photography, videography, cinematography, multi-spectral and hyper-spectral imaging with applications in areas such as ecosystem exploration and monitoring, precision farming, construction, infrastructure management, disaster and post-disaster response and relief, as well as exploration of remote sites.

UAVs have been extensively studied for use in remote exploration, including the documentation of archaeological sites [1]. In combination with terrestrial diagnostic imaging methods [2] to generate high quality 3D models of culturally important environments and artifacts [3], small multi-rotor UAVs in particular have proven invaluable for data gathering. One challenge is that they have to be launched from an open area in close proximity to the location of interest. Larger aircraft, on the other hand, can carry heavier sensor payloads such as LiDAR scanners [4] over much larger distances, yet may be difficult to deploy in the field. However, all current platforms are often handicapped by the need for pre-flight assembly and the availability of a clear launch

window. For example, the presence of a moderately dense forest canopy would serve as a practical ceiling for traditional platforms, with the platforms lift and control dependent on unobstructed rotors.

This thesis will present a an alternative UAV design tailor-made to address this issue through a ballistically deployed UAV platform, or Ground-Launched, Air-Deployable (GLAD) platform to be either projectile launched from the ground (figure 2.2) or inserted into the target environment from above via a 'parent' aircraft (figure 2.3). This gives it the ability to punch through sparse ground cover or be tossed clear of hazardous ground conditions such as turbulent winds, before deploying above. Furthermore, this thesis will look into new design strategies applied to the conception of such a platform: when designing a UAV with the very broad goal of facilitating deployment in field conditions, the widely differing operating environments which this infers are so broad as to make an ideal design for this job a superfluous notion: jack of all trades, master of none. Because of this, and the empowerment brought on by the decision to 3D print the platform, the thesis aims to suggest a new, more efficient design process for small ballistic 3D printed UAV platforms. By turning the conventional design process on its head, it is possible to turn it from one geared to produce a fully detailed one-size-fits-all design, to one where the final design is automatically adapted for field conditions. By creating a work-flow (figure 1.1) which allows for the individual optimization and design of each aspect of the GLAD platform's design, a single process can be used to design multiple platforms with varying designs for various applications in various environments. The idea is to use a process similar to multi-disciplinary optimization which can generate a platform in enough detail to be subsequently manufactured.

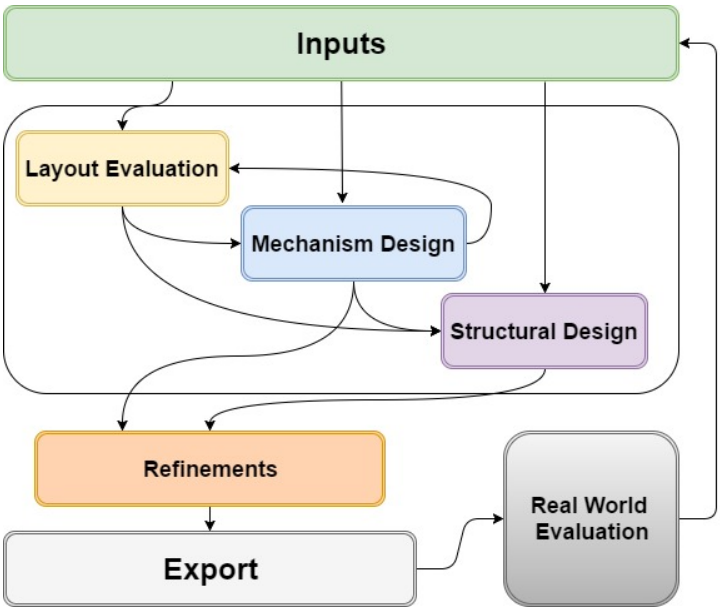

Figure 1.1: Diagram representation of the design scheme.

Chapter 2

Concept Development

2.1 Related Work

This thesis touches on many different topics, each of which are active research areas in their own right. These range from the design of UAVs for remote exploration, to biomimicry, to the use and implementation of design optimization methods for specific or multidisciplinary problems and lastly to 3D printing and the unique benefits it can bring to the manufacturing process.

2.1.1 Unmanned Aerial Vehicles

Unmanned Aerial Vehicles (UAVs) have known a meteoric rise in the past few years. Advances in miniaturization and batteries have made these platforms nearly ubiquitous in the world of surveying and exploration[1]. These platforms come in many shapes and sizes, with the two main categories being fixed wing UAVs and multi-copters.

The former function much like a standard airplane and offer long flight times and extended range, but due to their need to always move to generate lift, are not well suited for low level observations where static measurements are needed or tight spaces need to

be accessed.

The latter rely on the use of multiple vertical propellers to generate lift. Due to this active lift generation, they have much less endurance and range than their fixed-wing counterparts but make up for this deficit by gaining the ability for very precise control and the ability to hover. These qualities make multi-rotor platforms ideal for short range close-up surveying, or flights in tight spaces such as inside buildings and caves.

Other platforms exist which try to merge the advantages of both types of platforms, such as tilt-rotor UAVs which transition from a multi-rotor to a fixed-wing configuration mid-flight. Despite this, all of the platforms mentioned above share a key weakness: an inability to deploy in inclement terrain or conditions. One such example, common in the field of exploration or surveying, is the presence of a tree canopy overheard. Fixed-wing UAVs need some sort of runway to land and take-off, whereas multi-rotors can take-off vertically given a small gap overhead, yet without this clearing, the presence of any slight object in the rotor-blades' path dooms the craft to loss of control. A similar issue may arise in an otherwise suitable landscape in the presence of high winds: UAVs and aircraft are most vulnerable to turbulence near the ground as there is little room to correct for any sudden deviation.

These are two key issues which the GLAD platform aims to address by allowing the first and last stage of any flight to be entirely ballistic, meaning highly insensitive to the presence of light obstructions or unfavorable. Though the concept of ballistic launch of a UAV has been developed before[5], mostly for defense purposes, all previous developments have focused on the creation of UAVs which, once launched, change shape to becomes fixed-wing platforms. The decision for GLAD to be a multi-rotor platform in its flight form was motivated by its intended use as a short-range surveying drone.

2.1.2 Biomimicry

The concept of biomimicry is as old as engineering itself and consists of adopting shapes and mechanisms from natural organisms into a design that benefits from the efficiency emanating from evolution's many thousands of years of iterative design [6]. However, imitating nature requires the ability to create complex organic shapes, which lend themselves poorly to common manufacturing methods, where right angles and straight edges are the norm, a problem readily solved by 3D printing techniques. Combined with 3D printing's unique property of being a manufacturing process in which cost is independent of complexity [7], biomimicry was employed from the start in the design of GLAD in order to maximize efficiency and minimize weight. Though the drone, through many design iterations has lost its similarity to one specific natural object, many of the parts and details that make up the structure are based in shape or concept on biological sources

2.1.3 Optimization

Another key concept touched upon in this research, is the principle of optimization. Optimization in itself is a far-reaching concept which concerns itself with finding a "best solution" from a set of possibilities. This broad definition allows it to be used in almost any conceivable field. Most commonly, an optimization process modifies parameters on a model whose performance can be assessed. The creation of this model and the creation of the "fitness function" which evaluates the relative value of a configuration against another is one of the main challenges in developing an optimization program. Once this is done, many methods exist to find the desired solution. The most common is gradient descent, which assumes a very simple fitness function with a single optima. Yet design problems are often riddled with complex fitness functions which require more complex

methods to arrive at a good solution.

Evolutionary Optimization

Evolutionary algorithms attempt to solve optimization problems by mimicking the natural process of evolution. In this process, many different possible solutions are evaluated and the best are combined to produce ”offspring” solutions: solutions which share characteristics of both ”parents” with some random mutations. This is then repeated of a number of generations until the solutions converge to specific set of of parameters or ”genome” [8].

This method has been around for many years and has been used with great effect to solve problems ranging from airfoil selection to pipe design [9]. Evolutionary algorithms are very versatile and have been used in fields ranging from operations research, to physics. Due to their nature-inspired model they are also quite intuitive and easy to implement.

Despite their popularity, evolutionary algorithm fall short in a few areas. For one, they are computationally intensive, as they require an evaluation of the fitness function for every individual in every generation. They are also best used for problems with continuous, differentiable fitness landscapes, without plateaus, and are mostly used to find local optima. Because of this, the class of problems in which they can be used is limited.

Simulated Annealing

The second optimization method used in this thesis is simulated annealing. This algorithm mimics the process of crystallization in a cooling metal to find an optimum solution of the problem. When metal is heated and cooled, its crystal micro-structure will rearrange itself to minimize the amount thermodynamic free energy in the system [10].

It is this principle which simulated annealing mimics. Put simply, the algorithm jumps from a solution to a better neighboring solution within the search space, with a certain probability of settling for a worse neighboring solution, as time goes on, this settling probability becomes gradually lower. This means the algorithm slowly settles into the maxima or minima of the fitness function.

Despite the rather complex process it imitates, simulated annealing presents some unique abilities in the solution of optimization problems. The first of which being that it is rather simple to implement. The second merit of simulated annealing is its ability to find the global optima of a fitness function due to its ability to accept worse solution as it begins its search. This makes simulated annealing very capable in problems where other optimization techniques often under-perform: fitness landscapes with steps, discontinuities or very noisy definitions such as circuit board design or the notorious traveling salesman problem [10].

However a simulated annealing algorithm's performance depends on some internal parameters such as the defined "cooling rate" yet no magic means exist to deduce a good cooling rate when looking at a new problem. Thus most times simulated annealing has to be run a number of times with various cooling rates to find which one works best for the type of problem at hand.

Topology optimization

The last type of optimization problem this thesis will consider is topology optimization. Topology optimization problems are a class of problems where the program is tasked to find, within a defined search area, a topology to minimize a certain value, usually maximum stress or deflection, given a fixed amount of material. It differs from other optimization methods in that the solution is able to develop into any topology within the design space. It is usually run in conjunction with an FEM simulation to assess the

stresses or deformations at each iteration. This can be done in 2 or 3 dimensions.

Topology optimization is widely used in the aeronautics and aerospace fields where weight vs. structural strength is a crucial performance metric [11]. In these roles it serves to produce the optimal structure to resist certain loads with the minimum amount of material and is applied on both the large and small scale.

Despite the promises topology optimization brings to structural engineering, it comes with certain downfalls. As each iteration, a FEM simulation has to be run to assess the current iteration and therefore this type of problem is computationally intensive to solve and these problems are usually solved at a coarse resolution to speed up the process. Another shortcoming is that the solutions to topology optimization problems tend to be very organic in form, creating complex branch-like systems which do not lend themselves well to production through common manufacturing methods. For this reason, topology optimization is more often used as a preliminary design guideline, indicating the general shape of the member to be designed and where material is most needed[12]. This said, advances in 3D printing have allowed for the use of topology optimization as a full-fledged design tool since most 3D printing methods allow for the creation of complex, organic structures with no increase in cost and with very little modification of the analysis output [13] [14]. Because of this, 3D printers capable of printing topology-optimized metal components are becoming mainstream in the field of aerospace engineering [15].

2.1.4 multi-disciplinary optimization

The optimization methods presented above are usually applied to a specific problem, but the growing availability of computing power and the spread of optimization in design has led to a growing focus on developing multi-disciplinary optimization methods.MDOs allow for the optimization of large, complex designs encompassing multiple disciplines such as structures, materials or mechanical components. These

methods are becoming commonplace in the preliminary design of large ships or airplanes [16] where many subsystem must compete for space and weight allocation. These protocols have the advantage of allowing for a very comprehensive design to be created and evaluated but their implementation can be hampered by the complex nature of evaluating the relative importance of the various sub-systems. Due to their broad nature, MDOs are currently only used for preliminary designs, as relegating the detailed design of all sub-systems of a complex project to a single optimization program is a utopia with very little grounding in the realm of current or foreseeable possibilities. Yet this idea becomes more attainable when developing simpler systems such as the UAV platform studied here. The design process evaluated in this thesis can be described as an attempt to create a linear MDO scheme which concerns itself not only with the broader design concepts, but also the very details of the platform layout, structure, mechanics and manufacturing.

2.2 Possible Application Scenarios

The design process as well as the UAV concept presented in this thesis allows for the address of key hurdles in the domain of on-site surveying and UAV-based exploration. The novel design process and the use of 3D printing opens up new possibilities as to how and where these platforms can be designed and used, whilst the platform's innate abilities allows it to bridge a gap between existing capabilities of other multi-rotor and fixed wing UAVs [17]. In this section a few applications and scenarios are proposed to demonstrate some the unprecedented scenarios brought to the table by the design method, as well as examples of novel UAV uses brought about by the GLAD platform .

2.2.1 Adaptive Design and 3D printing

The whole concept of adaptive design, of having a design process which automatically goes through various stages of design optimization across multiple disciplines, arose from the need to create an array of platforms, which though similar in function were different in form. The platforms were initially developed specifically to enable researchers to more easily perform data-gathering in the field.

By using 3D printing as the platform's main manufacturing process (figure 2.1), it becomes possible to very easily obtain spare parts or perform repairs to any of the structural components by having access to a 3D printer anywhere in the world. Additionally, it also allows for new designs to be sent to the field instantly and manufactured on site. By reducing the delay between design and testing, it is possible to get near-instant feedback from the field as to what is needed. For example, a team conducting an aerial survey in the rain-forest could report that local tree heights are higher than expected and thus difficult to breach with the current design: almost instantly, the design can be reworked for higher strength and re-exported by email from a desktop thousands of miles away.

From here came to idea of automating this design-review process whereby someone in the field with no access to the outside could "dial-in" a new arm strength on the model to have the printer files regenerated. Pretty quickly, this turned into the design process which was developed: whereby arm strength, components size and many other factors can be taken into account by the model for the creation of a new optimal platform.

With this approach, a well defined adaptive model could be sent out to various teams working across a whole range of environments, urban, deserts, forested areas, with different missions priorities, height reached, package size, flight time. With this adaptive model in hand, each team would be given the ability to create their own uniquely adapted platform in the field, while changing some parameters and reprinting if the need arose or the conditions changed.

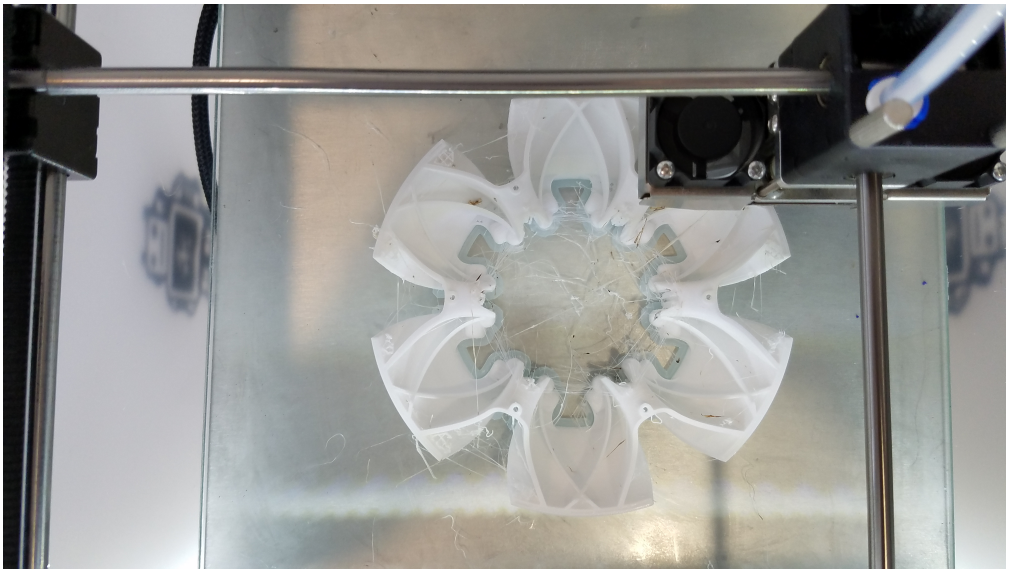

Figure 2.1: 3D printer printing a component of the GLAD platform.

One last conceivable field use of the adaptive model could arise in a scenario where a malfunction occurs rendering an electronic or mechanical component of the platform unusable. If this scenario occurs in present day, since the electro-mechanical components cannot be printed, the team would be grounded until a replacement part could reach them. Yet by giving the team an adaptive model, it allows for option of salvaging spare components from another platform, inputting those into the model and having the model generate a new platform capable of accommodating whatever spare part was found to be on-hand at the time.

These example cases show the benefits which can be brought about by a the use of an adaptive design process, and why such a process is particularly well adapted to scenarios where an small 3D-printable item or platform must be manufactured in small, highly specialized batches.

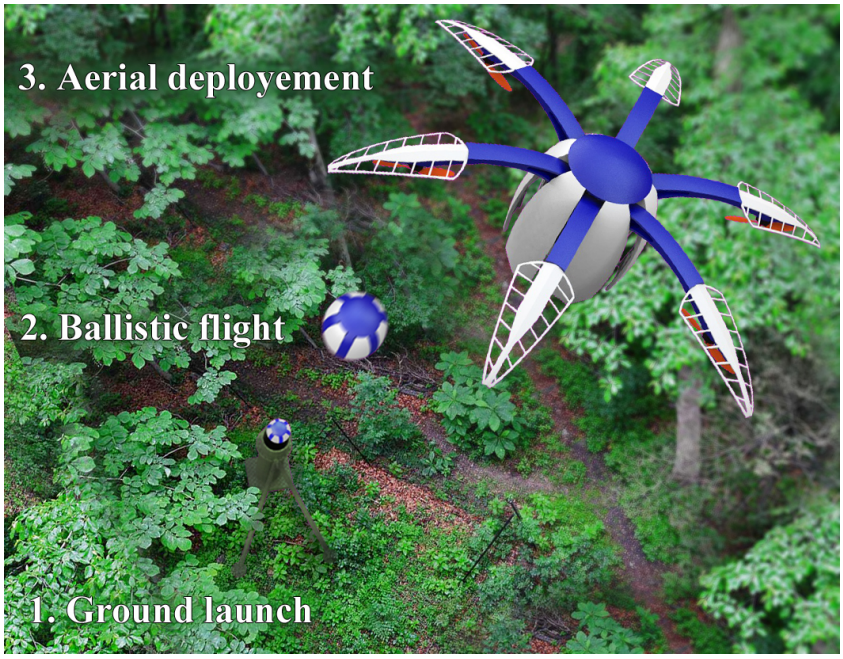

Figure 2.2: GLAD drone deploying from a wooded area.

2.2.2 Ground Launched Air Deployed

The main purpose of the GLAD platform is to serve as a ground launched platform which can be launched through a variety of means: from a football-style hand launch to a mortar-style barrel launch (figure 2.2). This platform's fast deployment in a steep parabolic arc allows for launch through forest canopies, narrow alleyways, skylight windows or other narrow openings with light obstructions.

This is a particularly useful characteristic in deployment from a forest-floor to get a bird's eye view of a location, or for post disaster relief where fallen wires, partly collapsed buildings and heavy dust might prevent conventional UAVs from deploying and thus providing high-level view. The use of a low cost UAV for post-disaster assessment is an idea that has proved to be a useful tool [18], but deployment is currently limited by the surroundings.

2.2.3 High Altitude Low Opening

Figure 2.3: Aerial deployment of the GLAD platform.

Another application for this re-configurable platform would be low-level deployment from a high-altitude 'parent' aircraft (figure 2.3). With minor changes to the software, the GLAD platform could be programmed to be dropped from high altitude in its folded configuration, only to deploy at some predetermined altitude, thus efficiently undergoing a large altitude change while protecting itself from high altitude weather conditions (figure 2.3). This approach would allow to relay a lower altitude aerial view of any point of interest below, saving the parent aircraft from the energetic cost and possible risk associated with a low pass. This gives the GLAD platform the ability to take an up-close look at any point which can be flown over with a large aircraft, thus extending

its reach to global proportions.In this scenario, recovery of the platform is unlikely, yet given that the platform is manufactured in a short time by a 3D printer with relatively cheap materials recovery may not be an objective. Furthermore the use of biodegradable materials one could make use of a platform without a large ecological impact [19].

In a scenario such as this one, it could be envisioned that after a large-scale natural disaster in a remote area, an airplane could be dispatched from hundreds of miles away to fly over the area at a high altitude while gathering site data. From there, the aircraft could release a swarm of GLAD platforms which would fall just short of ground level before deploying, spreading out to scan the scene for victims or risks from within a few meters of the ground, within an hour of the disaster first being detected.

2.2.4 Folding platform / small footprint

Other than enhanced deployment capabilities, the reconfigurability of the GLAD platform has the advantage of a decreased footprint (figure 2.4). Enhancing the practicability of transportation and long term stowing. One could have such a platform dormant in a folded position, protected from the elements and ready to deploy whenever commanded.

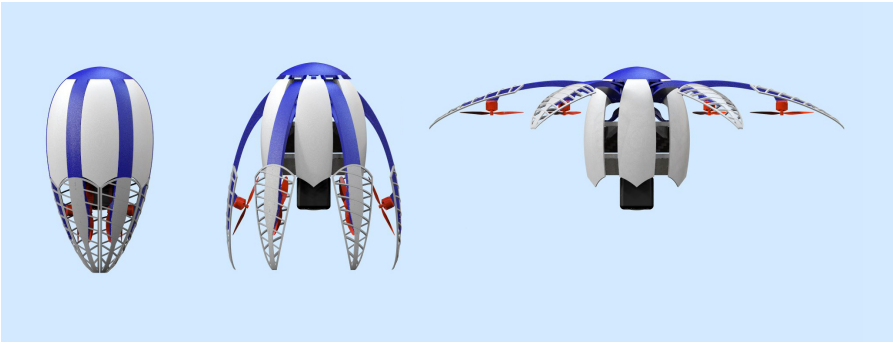

Figure 2.4: Rendering of a GLAD design in closed, shuttlecock and opened configurations.

One example of such a use could be a network of portable fire-watch stations,

containing a drone, launcher and a power source, deployed in various remote locations of a fire-prone landscape for months at a time. Upon registering faint signs of smoke from sensors on the station, such a platform could deploy and scan the area, relaying visual information to the proper authorities. Relaying data deemed useful to ecologist and conservationist [20].

Furthermore, a decreased footprint makes it more feasible to launch the multiple platforms using a single device. For example, a multitude of folding platforms can be stowed in a rocket-powered platform or a slightly larger UAV and deployed as a swarm in a moments notice. Thereby allowing for the deployment of a swarm of multi-rotor platforms to a remote location from a single platform or device. The concept, in broad form can also be extended to many other applications, such as planetary exploration or underwater platforms.

2.3 Preliminary Platform Design

Before setting out to create a process for the adaptive design of the GLAD platform, the concept itself first had to be developed and tested to ensure the soundness of the idea and assessing potential development hurdles. These hurdles are theoretical, structural, mechanical, aerodynamic and electrical. Below is a description of what challenges were encountered in the initial development of the platform, how these were approached and how they were eventually overcome.

2.3.1 Theory and conceptual design

On a very preliminary design level, the GLAD UAV was based on the use of biomimicry. The ”Egg” shape was chosen from the start since it possesses, on top of its evolutionarily-chosen structural resilience to impacts [21], great aerodynamic properties.

Additionally, biomimicry was used in the design of the propeller fairings which are made with light leaf-like veining for flexibility and high air-flow permeability. The concept's design then evolved around the need to support a range of versatile and at times unconventional ballistic launch options. To help quantify the required launch height it was decided that this height would need to encompass and significantly increase, the height attainable by a hand launch. Since the stresses in the platform are caused by the acceleration of the platform rather than by the target height itself, the launch method has to be considered. By including factors such as practicality and target applications, it was decided to base the launch stresses and launch height on the assumption of constant acceleration along a one meter long launch barrel. By emphasizing this over other factors such as air-friction (drag) and energy absorbed through deformation, the expected G-force on the platform can be estimated as a function of the desired launch height, considering Kinetic energy at launch and potential energy at the parabolic trajectory's apogee:

$$E_{Kinetic} = E_{Potential}$$
$$\frac{1}{2} * M * V^2 = M * g * h$$

Where:

$M =$ Drone mass

$V =$ Barrel exit velocity $= \sqrt{2 * a * g * L_{barrel}}$

$g =$ Gravitational constant

$a =$ Average acceleration factor (Gs)

$h =$ Max height reached

Simplifying, we get:

$$h = a * L_{barrel}$$

This means that our theoretical launch height (m) is simply the value of the average applied acceleration factor (G) on the drone multiplied by the barrel length.

With this information in hand and with the intent of clearing obstacles the size of small buildings or trees with a barrel length assumed to be around 1.5m [22], the goal G-force capacity was conservatively set at 10 Gs thus allowing for a theoretical launch height of 15 meters with a factor of safety of 1.6. This launch height, of course, does not account for factors such as air friction and deformations, so a lower actual launch height is expected for a given acceleration, a discrepancy which the factor of safety helps to account for. When launching from a barrel, a sabot can be provided to help distribute the force uniformly between all arms as well as ensure a close-to-hermetic seal between the projectile and the barrel walls. This sabot will also help diminish actual launch loads by deforming under the initial shock [23]. Additionally, tests will have to be performed on the electronic components on board the platform to ensure their ability to withstand these high G forces upon launch or set appropriate limits.

Having defined a benchmark loading for the drone, a conceptual design was developed. As mentioned, the retained design allows for a transition from an egg-shaped projectile to a hexacopter configuration via the unfolding of arms, which make up part of the folded shell. The deployed platform flies in a ”pusher” configuration whereby lift in provided by down-facing propellers. This decision was made in order to allow flight loads to push the airframe into a position of stable equilibrium, preventing premature folding of the drone at little energetic cost.

2.3.2 Structural Tests

Before any topology optimization was attempted, structural FEA analyses of the arms were conducted to validate the concept of launch loads being resisted by 3D printed plastic arms. These were conducted since the arms are the most structurally vulnerable

part of the design as they contain less material than the shell and are subject to axial and bending loads unlike the latter. This step was also crucial in the validation of the assumptions made about the 3D printed material used for the arm. 3D printed materials have a whole series of uncommon properties and therefore these must be taken into account when considering a 3D printed structure. Due to the vast variations in properties due to material or environmental factors, some baseline assumptions had to be made to accurately model the behavior of this material in these tests. To this end the 3D printed material properties were taken from Tymrak & al.[24].

The first analysis was a side-by-side comparison of two different arm designs. These compared an older version of the arm design to a more recent one with the intention of validating the maximum loads given by the FEA simulation. The two arms being roughly equal in weight, this also allowed validation of the relative structural efficiency of the new design. The arms were tested under in-flight loading conditions, where a load representing the motor thrust is applied on the motor mount, while the arm is restrained as it would be during flight. The flight load was calculated as follows:

$$F_{flight} = \frac{W * a_{flight}}{6}$$

Where:

F_{flight} = Applied force per arm

W = Drone weight = 11 Newtons

a_{flight} = Upwards acceleration factor = 2

Resulting in:

$$F_{flight} \approx 3.7 \text{ N}$$

The results for each arm are briefly summarized in figure 2.5.

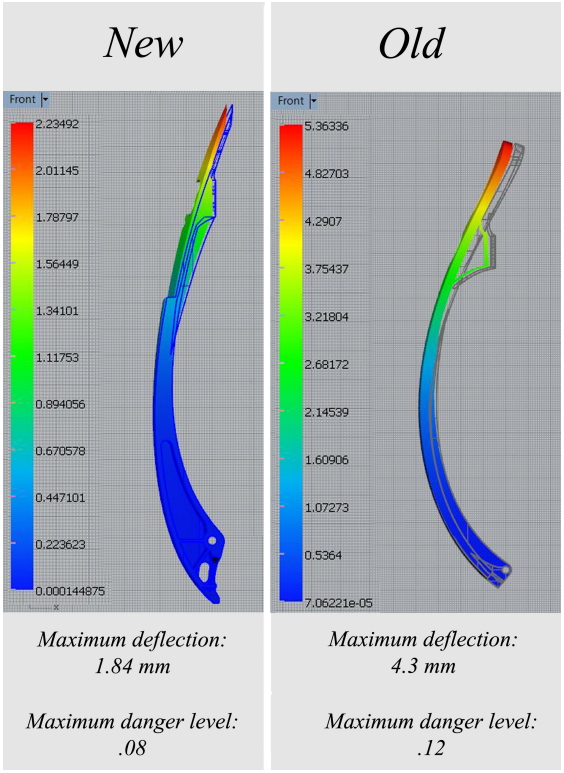

Figure 2.5: FEA deflection results summary

As shown by these results, the FEA confirmed the structural advantage of the newest arm design, which was rated as having 1.5 times the capacity and 2.3 times the stiffness of the previous design for equal weight. From there, a physical test was conducted on these two models to assess experimental stiffness and thus gauge the accuracy of the FEA prediction. The setup used mimicked the thrust load by weighing down the motor-attachment platform. The deflection was recorded for both arms and the stiffness derived as the slope of load vs. deformation as seen in figure 2.6. The physical test produced a stiffness values of 500g/cm for the old arm and 1,200g/cm for the new arm, giving a ratio of stiffness of 2.4 which falls satisfyingly close to the FEA stiffness ratio of 2.3, thus confirming the arm's ability to safely withstand the flight loads. Having validated the use of FEA for structural simulation purposes, another analysis was conducted of the motor arm under launch load. The loads for the arm at launch were

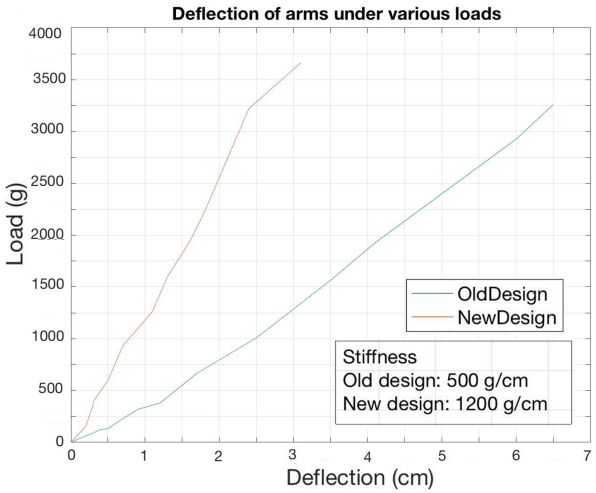

Figure 2.6: Experimental stiffness results from both arm designs

applied along the axis of the (folded) arm and distributed on its outer surface to mimic the load being spread by a sabot during a barrel launch. The acceleration was taken as 50 Gs instead of the planned 16 Gs to simulate poor load distribution which might occur in the barrel. The load was calculated as follows:

$$F_{launch} = \frac{W * a_{launch}}{6}$$

Where:

F_{launch} = Applied force per arm

W = Drone weight = 11 Newtons

a_{launch} = Design acceleration = 50

Plugging in the assumed values, we get:

$$F_{launch} \approx 92 \text{ N}$$

This loading cause the greatest danger level to the arm (.314) but proved the its capacity to withstand the launch (figure 2.7). Despite this, should a 50 G load actually be

applied to the arm, the survival of the hinge connection and thus the platform could not be guaranteed.

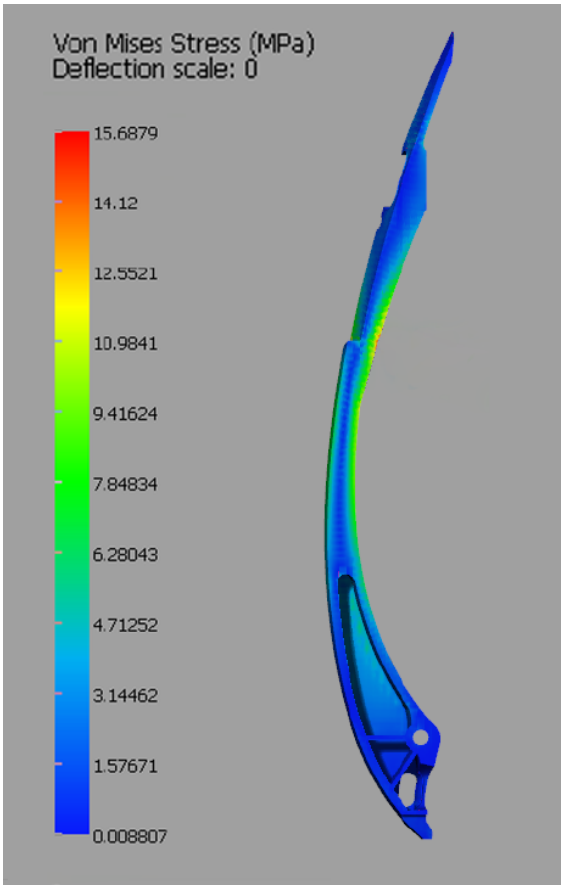

Figure 2.7: FEA result of arm at launch.

2.3.3 Mechanical tests

Having shown the GLAD platform could survive a high-G launch, it was necessary to develop a mechanism by which the platform could transform from a projectile to a flying platform. This transition needs to be fast and decisive as anything short of swift and full deployment would doom the platform to continue along the parabolic arc it began until its very unfortunate end. The mechanism also had to be compact and lightweight so as not to affect the drone's capabilities and overall shape.

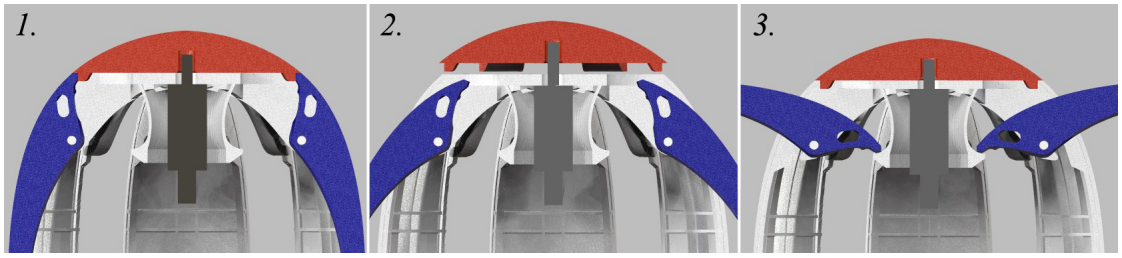

Figure 2.8: Solenoid and spring release mechanism initially considered

Various types of mechanisms were considered: from individual servos allowing independent control of arms to compressed air systems, but these proved too cumbersome, too weak, too power hungry or too complex (figure 2.8), and thus a brand new idea was put forward. By making use of 3D printing's innate ability to create complex shapes, a mechanism consisting of a single revolving grooved gear was devised (figure 2.9).

The resulting doubly curved helical gear, also referred to as the hyperboloid, provided a way to rotate all six arms around their respective axes, in a fully controllable manner while using a single stepper motor aligned with the principal drone axis which rotates a single moving piece. The ability to use 3D printing to seamlessly manufacture a complex geometry such as this one, makes the hyperboloid gear a very attractive and novel solution to the problem. Additionally, The use of pin following grooves instead of gears also allows for more uniform stress distribution in the part as there is constant contact between the arms and gear. Finally, it prevents any of the gears from skipping and becoming out-of-sync with the other arms. This detail ensures that a failure to open leaves the platform completely self-enclosed, lowering the risk of a partial-opening which would be more catastrophic for the UAV.

Altogether, this design provides a more efficient, functional and elegant opening mechanism than the initial spring-loaded idea. [25].This mechanism was built and tested to confirm the GLAD platform's ability to transition from its ballistic configuration to its flight configuration using on-board power.

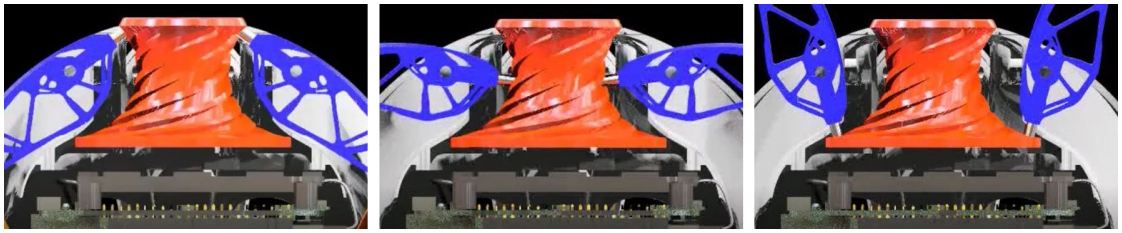

Figure 2.9: Tryptic of an internal view of the platform transforming, showing the hyperboloid mechanism (red) and the unfolding arms (blue).

2.3.4 Aerodynamic tests

Figure 2.10: Qualitative hand-launch testing to establish ballistic flight behavior.

Another concern in the design of this platform is its aerodynamic behavior. Due to the standard multi-rotor layout of the platform in powered flight configuration, flight behavior was not deemed a concern in the opened position. However, successful and stable ballistic flight of the platform is key in maximizing height attained, efficiency and successful deployment of the platform and therefore requires careful consideration. Due to the fact that changing the platform's aerodynamics would require changing the design

in major ways, it was considered inefficient to conduct ballistic flight tests with a finished model at the end of the design process. To this end, a dummy model was created to be printed entirely out of plastic, with the same external shape as the current design but with thicker walls of varying width to correctly account for the mass and center of gravity of the various electrical and mechanical components removed from the dummy model. This method allows for easily made and disposable test platforms.

Since flight characteristics are not easily quantifiable, these test were done rather arbitrarily simply by tossing the model through the air and getting a sense of its in-air behavior (figure 2.10).

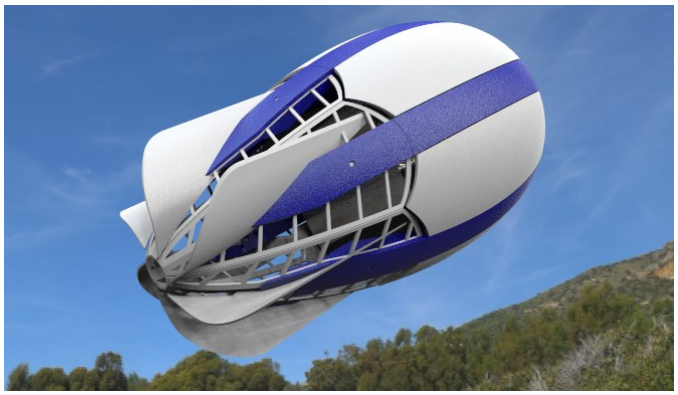

Figure 2.11: Fin concept for spin-stabilization.

It was found that by hand launching, the football-like shape of the GLAD platform lent itself well to a hand-induced spin, leading to a stable flight through the air. However it was discovered that without this spin, which would be harder to induce in a barrel launch, the fairings over the propellers produced little in terms of drag, making the platform prone to tumbling.

These tests showed the necessity for fins or similar drag-inducing fairings on the rear of the platform to stabilize it in flight (figure 2.11). Alternatively, a more careful design could achieve a platform for which the location of the center of pressure falls behind that of the center of gravity in the direction of travel. Due to the relative simplicity

of the former solution and the necessity to redesign parts of the drone specifically for the latter, this modification will be addressed once hand-launch, air-opening and flight had been successfully demonstrated and a specific barrel launch method is agreed upon.

2.3.5 Flight software development

The last step in achieving successful flight and deployment of the platform is the development of a flight control system for the GLAD drone. The control system is designed structurally and electrically around the BeagleBone Black as well as the Robotics cape created by Strawson Designs. The software environment for GLAD is the same used throughout the UCSD DroneLab to maintain interoperability. Which uses pulse width duration to communicate with the speed controllers. The flight software operates under the same architecture a typical hobby drone might, with the exception of a few tweaks to link free fall detection with the firing of the stepper motor responsible for unfolding the six arms. In short the flight protocol calibrates and initiates all speed controllers and components, but waits until the accelerometer detects near zero acceleration in the Z-direction, which triggers the opening mechanism, before driving any of the motors. Since the control system is based on a Linux operating system it is easy to connect the GLAD drone with a wide range of sensors and network interfaces. Though this is in the periphery of this thesis's scope, an overview is key to understanding how the platform will be able to deploy and sustain flight.

Chapter 2, in great part, is a reprint of the material as it appears in "Towards Bio-Inspired Structural Design of a 3D Printable, Ballistically Deployable, Multi-Rotor UAV", *IEEE Aerospace Conference*, 2017. Luke W. Henderson, Twain Glaser, Falko Kuester. The thesis author was the primary author of this paper.

Chapter 3

Optimization of the GLAD design

3.1 Adaptive Design Concept

Having broadly defined the conceptual design of the GLAD platform. The challenge now lies in optimizing this design process to fit the various deployment scenarios as described previously. The linear multi-disciplinary optimization scheme can be presented as a succession of 6 major steps. Each of these steps should be thought of as independent optimization processes which, given a series of inputs, will provide one or more outputs to be passed on to the next step. One of the main challenges is to ensure that these processes, or ”phases”, are flexible enough to generate a coherent output given a range of input. Without this flexibility, there is a risk of error propagation from one step to the next leading to a non-coherent final output and wasted computation time. This methodology lends itself particularly well to implementation within a graphical programming environment, such as Grasshopper for Rhino used for this optimization process, where the input and output of every sub-routine can be traced to the next. The 6 main phases proposed for this protocol are the following:

Input Parameters

This first phase serves as the user interface, it is here that all the required parameters for the design are inputted. In this case, this entails such inputs as the motor type, propeller size, controller type, payload size and shape, maximum barrel diameter, launch force, mechanism opening limitations such as deployment time or torque, or finally whether a hexacopter or quadcopter design is desired. In this phase, many other ”sub-parameters” are also defined which control the behavior of the other phases to be tweaked during development. In the early stages of development, it was considered that this phase might be replaced by a parameter optimization phase which would decide the best combination of the above options given the mission description and a list of available hardware and electronics. However, though this is no doubt feasible, the added benefits of such a phase for a demonstration process such as the one developed did not outweigh the complexity of generating such a process and thus, the phase produced assumes the appropriate components are correctly chosen by the user.

Layout optimization

The second phase in the chain uses the information passed on by the first phase about the component geometry and the physical size and shape requirements to optimize the location of the various components. Due to the GLAD drones folding design, quite a large amount of freedom is given to the placement of components when folded. That said, some limitations were put forward to allow for the vast simplification of the optimization functions search space. These key assumptions about the general layout revolve about two key decisions:

Axial Symmetry – The platform is assumed to be axially symmetric, from the motor and propeller positions to the outer shell. Though this requirement is not a strict necessity to the functioning of the platform, it is conform to the idea of a barrel launch

and doing otherwise would require separate analysis of each arm and possibly further tailoring of the flight code and opening mechanism.

Vertical layout–The general organization of the platform along its vertical axis is fixed: the opening mechanism sits below the controller board, above which is the battery, followed by the payload. Though the orientation of those components is subject to optimization, this general rule allows the optimization process to rule out cases which, though space-efficient, would most likely be unpractical.

Given these assumptions and the geometry of the various components, the layout optimization phase goes about figuring out the best way to organize the different parts inside the shell and the shape of the shell.

Mechanism Design

In this third phase the optimization process makes decisions about the layout, size and placement of a key component of the GLAD platform: the hyperboloid shaped opening mechanism. Despite having decided on a fixed type of opening mechanism, the hyperboloid concept can be adapted in many ways, such as: the number of arms, the available servo torque, opening time and opening angle of the propellers, and these are decisions which must also be optimized due to their essential nature within the GLAD platforms function. The mechanism optimization phase must take inputs from the layout of the components such as the shell outline and propeller angles when folded, as well as the opening requirements from the input phase. From these, the optimization process decides not only the best radius and orientation of the mechanism face but also the placement of the arm hinges which dictate its shape and the movement of the propellers.

Structural Optimization

Having the location of all the main elements defined, the fourth phase is charged with the design of the platforms structure. This in itself involves two key elements: the folding arms and the drones mainframe. To make these decisions, the phase must take as input the location of all the components and independently decide where boundaries between the various parts should be. Additionally it must be able to take or calculate the loads to be sustained by the structure before performing the optimization.

Refinement and model generation

With the main structural elements designed, and the component layout set, this phases work is to add finishing touches from making the correct screw holes in the correct locations to generating a full 3D model of the hyperboloid and other details which were only loosely defined in the other phases. It is this step of the process which differentiates it most from conventional MDO programs.

Export

The final phase is tasked with preparing all the parts defined previously and preparing them for export to a 3D printer. It performs administrative tasks such as saving and labeling the various files, isolating the various components, arranging and best orientating them for printing. These phases, illustrated below, constitute the main steps of the optimization process put forward in this thesis. Due to the computational weight of each of these phases, they have been arranged so as to allow for user review of the solution before moving on to the next step. This ensures an erroneous result is caught instead of being passed on uncorrected. For each of these phases, we will explore their logic and the intermediary phases which compose them and serve to properly reorganize the inputs and outputs to ensure smooth-sailing.

3.2 Optimization Implementation

The whole premise of the adaptive design process is the idea of generating a design dependent on a set of inputs in a user-friendly way, and therefore the first step in creating this optimization process is to define the inputs.

The input phase is presented as a simple set of sliders and drop down menus presenting the various options available to the user. These various inputs can be categorized into 3 main categories: Primary numerical inputs, class inputs and secondary numerical inputs.

Primary numerical inputs represent the major and simplest design decisions and consist of sliders or drop-down menus which offer the option to pick a given number. These numbers represent choices such as the battery width, height and length dimensions, the maximum allowed platform diameter, the expected launch force or height and the 4-or-6 rotors design decision.

Class inputs are so-called because, despite their presentation as single items to be picked from a list, they represent a whole range of data. For example, when selecting the type of PCB from a drop down list, the user is actually specifying a geometry, along with the screw hole configuration and associated data. These class inputs cover other major user decisions such as propeller type and size, servo type, motor size, PCB and Payload. Each of these options, behind-the-scenes, selects a combination of items. The content of the classes is defined within the optimization process to simplify user interface, with the option for the user to enter his own geometry and associated data by choosing, for each of the fields, the ”custom” option.

The last type of input, secondary numerical inputs, are of the same type as primary numerical inputs in so far as they set, within the optimization process, a certain constant to a certain value. However, unlike their primary counterparts, these are not shown on

the interface and are inputted inside the different phases as they are intended for more detailed refinement. These control a whole range of internally preset values such as internal mechanism clearances, design safety margins for launch loads, propeller arm thickness etc. Due to the large number and small relative impact of these values, they will be left out of most diagrams presented throughout this thesis.

3.2.1 Layout Optimization

As described previously, the layout phase serves to find the best orientation of the various mechanical and electronic components of the platform in the folded state. To this end, the layout phase takes as input most of the parameters specified in the ”input” phase: the number of propellers, the geometry of the propellers as a 3D model, the geometry of the controller board, the geometry of the propeller motors as well as the mechanism opening servo, battery dimensions, the geometry of the payload and lastly the maximum required barrel diameter. The inputs are accompanied by internal optimization parameters. These internal parameters control the position and tilt of the motors/propellers, as well as the orientation of the electronic components on the platform.

Having defined these inputs, the layout phase can be further divided into 8 sub-stages which jointly work on these inputs. The first 5 of these sub-stages are simply concerned with generating a mock-up of the model for the analysis of the design. For example, the first sub-stage takes as input the 3D geometry of the PCB and the rotation information for the PCB defined by the internal inputs, and simply outputs the 3D geometry of the rotated PCB. The other model-generating sub-stages perform similar actions with the battery, the servo motor and the payload, taking the additional care of ”stacking” the resulting geometries: if a thinner PCB is defined, the battery should be lowered and not remain where it would have been had a thicker PCB been defined.

The 6th sub-stage takes as input the rotated and stacked geometries of all the

components and checks the various models with one another for any intersection or overlap of the different geometries and outputs the total intersection volume to be used in the 8th sub-routine.

The 7th sub-stage is the one in charge of generating the shell profile for any given layout. Indeed, to best assess a design, an overall shape of the drone must be guessed from the internal components layout. This outline must reflect the necessarily streamlined shape of the platform and thus cannot be defined as a simple rectilinear envelope. These are the type of definition challenges that are key to optimization and make the definition of the problem such an important part of the problem-solving process. A brief description of the shell outline generation process is that the main protruding features of the components are located to define, via the creation of a convex hull, an area which the shell must avoid. This outline is then offset for member clearances and refined a few times to generate a smooth, shell-like curve which efficiently contains all of the elements as laid out. This outline, once revolved creates the shell geometry, which is outputted along with its volume.

Finally, the 8th sub-stage of the layout phase is the all-important ”Design score”. This sub-stage takes the outputs of all the other sub-stages to assess the layout in its current form and produce a numerical ”score” for the optimization process to assess and minimize. Due to its importance, it can be considered as the core of the layout phase. To assess a layouts performance, one must define what a good layout is. For the GLAD platform, a good layout was defined by laying out basic rules such as not allowing any overlap between components, ensuring all the physical limits, such as maximum barrel diameter, are respected, and finally attempting to minimize volume or surface area of the final shell. Given these guidelines, it becomes possible to score a given layout by accounting for volume and adding penalties if one of the constraints is exceeded. That said the definition of this score must be done with the optimization protocol in mind to

maximize convergence.

This brings us to the optimization, which is performed by allowing the optimization program to vary the layout phases internal inputs and assess the resulting ”design score” to find the best possible layout. The optimization method chosen for this step of the design process is evolutionary optimization. This was chosen due to the relative continuity of the search space, where a small adjustment in the rotation of a component, is expected to have a small influence on the design score, yet the larger-scale complexity of the fitness function prevented the use of simple gradient descent. Due to evolutionary optimizations previously define sensibilities it was important to define the scoring function in a way which minimized ”plateaus” in the search space.

This type of search space results from having, for example, intersections penalized by an added 9000 points, this helps the optimization process favor a layout with no intersections but leaves it indifferent to two different layout with varying level of intersections. For this reasons, the design score function was tweaked to account not only for the presence of an intersection but for the volume of that intersection, with a penalty of the type:

$$P = 9000 + (\text{Volume of intersection}/20)$$

The resulting search space along a sample unique parameter is illustrated below (Figure 3.1). Much like a marble following a slanted track, the optimization can here ”find” the lowest score with greater ease.

The final function used for the assessment of the platforms layout was the following:

$$Score = \frac{V_s}{10{,}000} + \delta_{cyl}(5{,}000 + 10R_d) + \delta_{V_int}(1000 + I)$$

Where:

$V_s =$ Shell Volume in mm

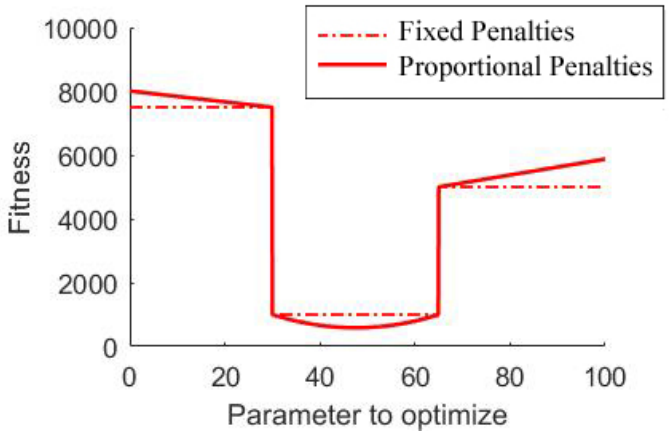

Figure 3.1: Single dimensional example of a properly defined fitness function where proportional penalties help "guide" the optimization.

δ_{cyl} = Boolean corresponding to the radius limit rule

R_d = Platform radius at widest point

δ_{int} = Boolean corresponding to an intersection

V_int = Intersection volume

Through these definitions, the layout phase is able to generate a coherent component layout for a wide range of components given a variety of restrictions before passing the given layout on to the next step of the design process.

3.2.2 Mechanism Design

Having laid out the drone components in 3D space, the mechanism design phase comes into play to create an opening mechanism which best suits the geometry of the platform. A few parameters dictate the shape of the hyperboloid: the location of the arms hinge, the radius of the mechanism from the hinge location to the gears surface, and the angle of rotation. The properties of the grooves, such as the pitch are not defined in this phase but rather in the refinement phase. Of those parameters, only the angle of rotation is an external parameter, as it is dependent on the final angle of the propeller

in the folded stage as decided by the layout phase. The other parameters are created within the mechanism design phase to be optimized. The shape of the mechanism itself is defined quite simply by a hinge location and an arc of the given radius drawn about the hinge. To generate the mechanisms shape, the arc is rotated about the drones central axis. Therefor the mechanism design phase concerns itself only with finding a suitable hinge location and appropriate arc. Similarly to the layout optimization phase, the definition of a ”good mechanism” must be stated by defining guidelines.

The first design guideline insures sufficient clearance by verifying that, at its closest point, the arc must be no closer than certain predetermined distance from other components such as the servo or the PCB to allow for clearance and account for yet-to-be designed structural members between the components and the mechanism. These distances are arbitrarily defined as secondary design inputs.

Other simple yet key guidelines are that the hinge must be located within the shell and that the arc length must be greater than a certain value to allow room for enough grooves to be placed into the mechanism, depending on the thickness of the pins used, the number of arms and the pitch of the grooves.

Lastly, it must be insured that, When in the open configuration, the propeller arm must not intersect with the mechanism. In other words, there should be a gap between the arm and the lower part of the mechanism when open. As a secondary goal, this gap should be as small as possible for aesthetic reasons.

Given these rules and our inputs along with a handful of other arbitrarily preset inputs such as the minimum clearance between the mechanism and the PCB or the safety factor added to the length of the arc to account for material at the start and end of the groove, it is possible to write a program to assess the aptness of any given mechanism design. This task can once again be broken up into sub-routines performed within the mechanism design phase:

The first subroutine simply takes the inputs of hinge location, radius and preset inputs to generate the current arc.The second utilizes the shape of the shell defined in the layout phase to simulate the arm when rotated about the suggested hinge by the suggested amount.The third sub-routine estimates the distances between the arc and the PCB and the arc and the servo to score the mechanisms adhesion to the first rule set above.Lastly, the 4th, 5th and 6th sub-routines respectively score the mechanisms adhesion to the minimum arc length rule, gap rule and hinge-within-shell rule.

The results of the four scoring subroutines are then added to generate the final mechanism score in its current configuration. Here again, similar to the method used in the layout scoring, score penalties are given as a function of the distance to prevent ”plateaus” in the search space. This, in turn, is used by the optimization protocol to assess and adjust the design of the mechanism. For the shape optimization of the mechanism, simulated annealing was chosen as the method of choice since the search space is quite irregular and early attempts with evolutionary optimization yielded many ”locally optimum” cases which could not be implemented.

This ”fitness landscape” refers to the variation of the design fitness depending on the three parameters being optimized, here: Hinge X location, Hinge Z location and the mechanism radius. To help visualize this, the radius can be fixed and the fitness landscape becomes 2 dimensional, along the X and Z axis of the hinge location. Therefore we can map the fitness of the design, for a given radius, according to the placement of the hinge (figure 3.2). In this figure, the color indicates the fitness of the solution, with dark blue representing a lower score and therefore a better solution, while light blue, green, brown and white represent, in turn, progressively worst hinge location of the given layout and radius. The red lines indicate the location of the hinge, which is currently located at the global minimum, as well as the arc which defines the mechanism and two curves which represent the arm’s exterior outline before and after rotation. The map seems to

show areas of uniform fitness, yet these are actually due to the fact that one or more large design penalties kick in those areas, thus the stark difference in penalties dims the slight gradient which exists in each of those regions. Another important information this figure reveals is that, though all the best solutions seem to be confined to a single basin, a small local minimum exists away from this basin where the true global minimum is actually found. Whereas evolutionary optimization would most often fall happily into the larger basin, the use of simulated annealing allowed to find the non-trivial global minimum.

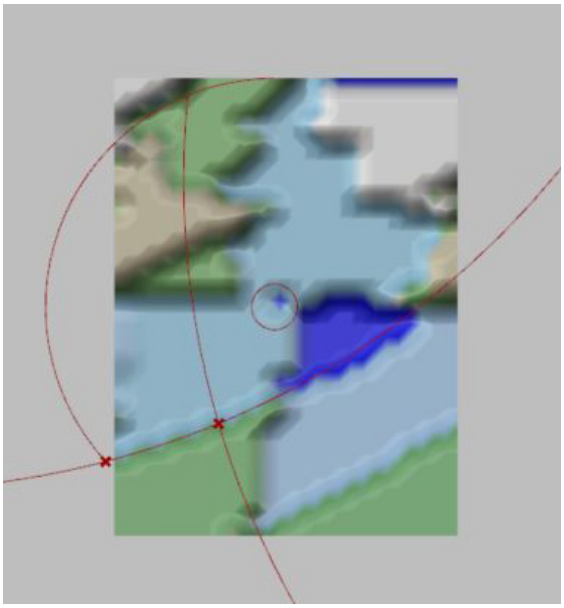

Figure 3.2: Illustration of mechanism fitness function for a fixed radius.

3.2.3 Structural Optimization

With the platform layout decided upon as well as the mechanism size, layout and hinge locations set, the platforms structure can now be developed. The structural phase is one of the most complex phases in the design process. Its role is to decide on the outline and shape of the various structural members and the structure which composes them. The 2D and 3D topology optimization used in this optimization process is run through a plug-in program which takes as inputs the boundary region or volume within which

the optimization can take place, the load region, support regions, areas to specifically avoid and the loads to which the structure is subjected. Of these, the easiest to obtain are the launch and flight loads as they are either defined by or easily deduced from the inputs. The challenge in this phase is the definition of boundaries for mobile structural elements within a larger platform which, itself, has a dynamic layout, prone to change with every new design. To do this, certain rules have to be deduced as to the interaction and relative placement between components. This general philosophy can be illustrated by explaining further some of the rules and assumptions made in the definition of the foldable arm boundary:

The first boundary defines is the outer limit for the arm geometry which is the defined by the outer shell of the drone for obvious reasons.The lower part of the arm where it interacts with the mechanism can then be defined by a curve slightly offset from the mechanism profile. The circular arc of this curve centered on the arms hinge guarantees the concentricity of the arm and mechanism during all phases of the opening. To avoid the main internal components, bounding boxes are created for each item and the vertices are identified before being rotated into the plane of construction. This method allows to simplify the creation of the arm region should the geometry of the payload or PCB be complex. The rotation of the vertices in the plane of construction also guarantees that the arms will not intersect the components no matter the number of arms set in the inputs.Avoidance of the internal components is simplified by their known stacking order, defining the border to stay outside the propeller region however, is more complex. This is done internally by identifying a few of the possible layout cases as they relate to propeller placement relative to the internal components, which allows to optimization process to make an outline selection accordingly. From these assumptions, the various limits defined are joined to one another to form a boundary by the closest point method or other method shown in figure 3.3. Having defined the boundary of the arm, the location of the support

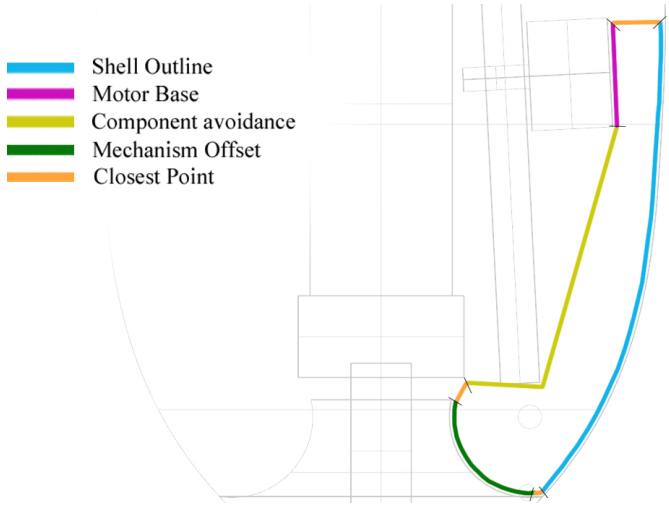

Figure 3.3: Sample arm outline annotated to illustrate the generation method used for each edge.

(hinge and mechanism pin) are easily located as the hinge location and mechanism start position are known. Next, the flight load is easily defined as being applied by a rectangle at the motor base in a direction normal to the propeller orientation, and the launch load is applied at the top of the arm. This complex definition of the region in which the arm can be created permits great flexibility, allowing the optimization process to create an arm for a wide range of conceivable layouts. Various resulting regions, prepared for the 2D topology optimization are shown in figure 3.4. From there the 2D topology optimization

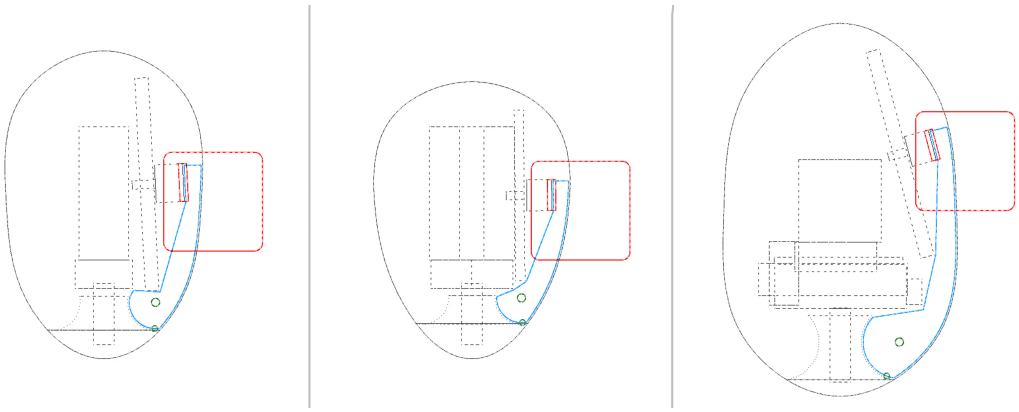

Figure 3.4: Sample arm boundaries resulting from different configurations, showing the load application areas (red), optimization limits (blue) and supports (green).

is run, yielding a pattern in the defined region varying in density from 0 to 1. This is output is further processed by selecting only the areas in the regions where the value is greater than a certain threshold, performing further smoothing and trimming operations, adding a hole for the hinging and mechanism pin, before extruding the outline to form the arm. This method of extruding the result of a 2D topology optimization was chosen for the arm due to the fact that in this member, the forces and supports are all readily aligned in a plane. Additionally, this method greatly reduces precious computation time and facilitates 3D printing of the arms, due to the two flanks of the extrusion being flat and level. the results can be seen in figure 3.5.

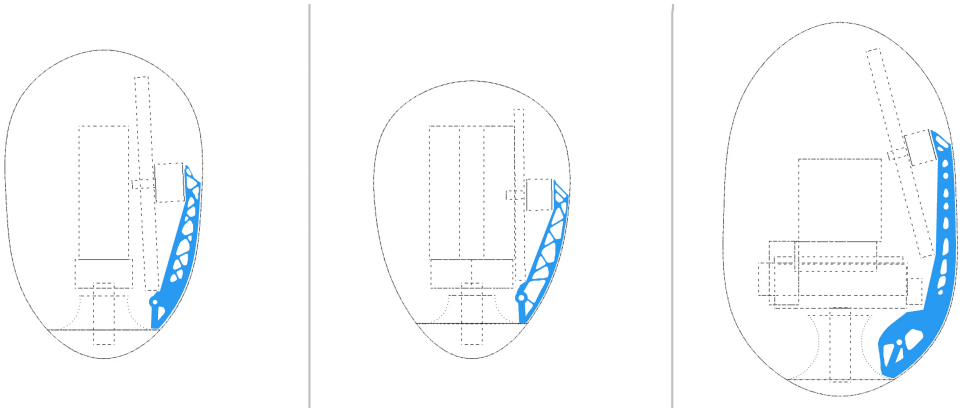

Figure 3.5: Arm designs resulting from 2D topology optimization and processing.

The topology optimization for the body of the structure follows a similar process and manages to be both simpler and a lot more complicated: the definition of the optimization loads and volume are simpler, but the computational weight of performing the optimization is almost prohibitive. Indeed, for the topology optimization of the structure, 3D topology optimization has to be used due to the non-planar nature of forces and components. The main forces being resisted by the structure are: the launch force, applied on the top half of the structure, the mechanism torque, being applied at the servo and a slight uniform outside pressure defined on the entire outside shell to simulate

handling. The optimization volume is simply the outer shell as previously defined. On top of that are added ”no-go” regions where the optimization process should not seek to put any structure: these are simply the bounding box of the various components and the mechanism with some clearance. Lastly, the structure must also not get in the way of the unfolding of the arms, despite the seemingly complex nature of that problem, having defined the arm, propeller and motor geometry and knowing the exact angle and center of rotation of the arm, we can easily create a sweep volume to be avoided by the topology optimization. Therefore defining loads and volumes for the optimization to run is within reach.

Unfortunately, by nature, 3D topology optimizations computational weight increases with the cube of the number of elements uses (O3). This severely limits the optimization processs performance by either limiting the resolution of the optimization, and thus yielding a result too rough for correct implementation, or by increasing the computational time beyond anything practical. For satisfactory resolution, the program should be able to run with voxels of about one half-millimeter, yet at this resolution, a quarter scale analysis run on a standard laptop took approximately 3hrs and 30 mins to run. Therefore suggesting that a full scale analysis, 4 times the size and therefore 64 times the computation time would take around 9 days, 8hrs to complete. Due to this hardware limitation, the optimization of the structure is approached more theoretically in this thesis than that of the arms structure. A sample result for the structure created by coarse topology optimization before being manually refined is shown in figure 3.6.

3.2.4 Refinement

Having covered the main optimization phases of our adaptive design process, the two remaining ”house-keeping” phases will now be discussed in more detail. As previously mentioned, the role of the refinement phase is to take the geometry created

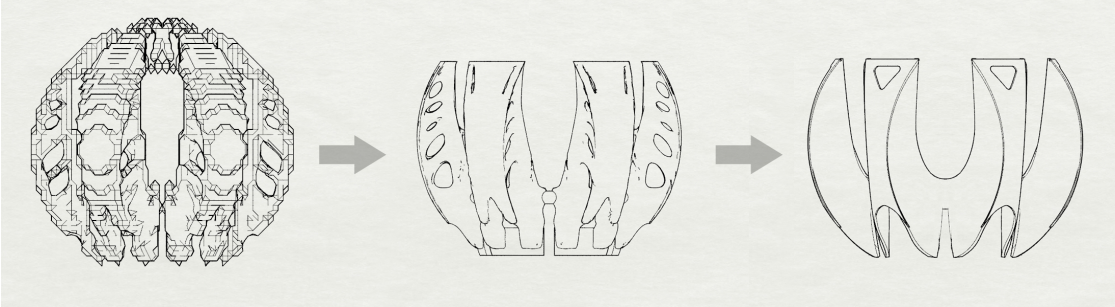

Figure 3.6: Sample output of the 3D topology optimization. From left to right: Output of a coarse optimization, smoothed result for the central section and interpreted result of the central section.

in previous phases and turn it into a better defined, and assembly friendly model before export. Due to the finicky nature of this task, it is perhaps the phase whose various roles are most loosely defined and the one which is most often tweaked to match unforeseen design intents. To simplify the description of this phase, it will be summarized by describing the 3 main tasks it accomplishes: Building a 3D model of the mechanism with spiral grooves and other attributes, generating screw holes for the assembly of the structure and the fastening of the components, and finally dividing the structure into various sections to facilitate assembly.

Structure slicing

The first of these processes, and the easiest to implement is the slicing of the structure into sections. From experience working on this type of platform it has been found that the structure is best separated longitudinally into 3 sub-sections (Figure 3.7). The central section protects the internal electronics, PCB and servo. The lower section is removable and allows for the easy installation of the mechanism and the propeller arms. The third section is the top section which contains the payload, allowing for easier access and interchangeability, and when closed keeps the internal electronics sheltered from the launch force. The location of the separation is relatively straightforward: the

lower and central section are divided by a horizontal plane passing through the arm's hinges to allow it's installation to lock the hinges in place. As for the top and central section, they are separated by a horizontal plane which corresponds to the top of the battery. This allows the battery to be secured by the top attachments. The use of simple horizontal plane to separate the various sections arises from the need to easily 3D print these sections, by doing so each section has a large flat surface which can be laid down on the printer bed for better printing. The different sections are secured to one another with screws.

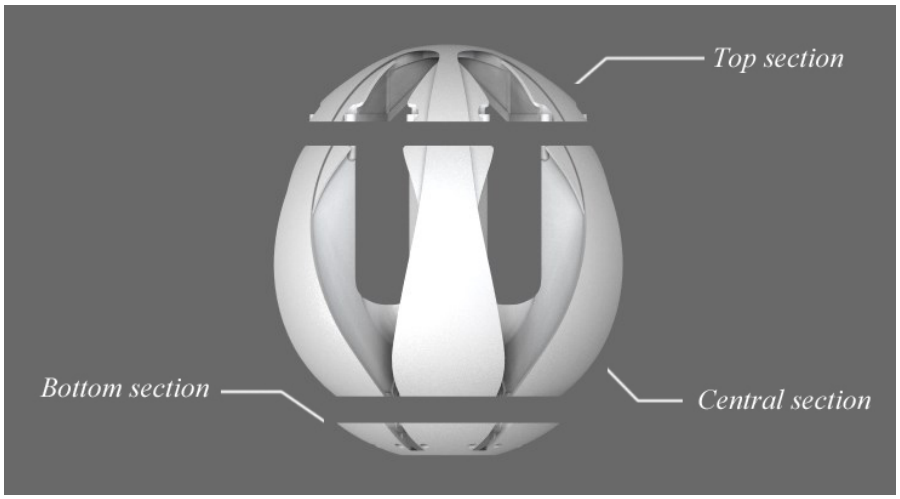

Figure 3.7: Top, central and bottom slices of the structure.

Screw holes

The next step in the process is the insertion of screw holes for the various attachments throughout the model. The challenge of inserting all the holes for assembly is mainly one of bookkeeping. Indeed, most electrical components such as the PCB or motors come with screw holes in preset locations and orientations. These must be defined in parallel with the component geometry, as secondary inputs in the input phase. By keeping track of all transformations applied to the various components through the design

process, and by subsequently applying these transformations to the corresponding screw holes, the final correct location for the holes can be obtained. Having the final location and direction of all the screws, these can be formed into the model. In this respect, the design studied here presents two advantages: all screws used throughout the model are identical (M2x6), and 3D printed plastic is particularly well suited to ”tapping”. These advantages mean we can define a single ”typical” cylindrical hole to be applied at all the tracked locations. With that said, different screw sizes could easily be accommodated by keeping track of the screw type in our bookkeeping exercise. Therefore, by keeping track of item screw locations and compounding the transformations undergone by our geometries, we can ensure the proper placement of screw holes in the drones arms, and structure.

Hyperboloid model creation

The third item whose creation is addressed by the refinement phase is the 3D model of the mechanism. Though this geometry could very well be created along with the mechanism design decision, creating it further down the design process prevents the optimization process from attempting to recreate this complex geometry at every iteration of the mechanism design optimization.

In short, the hyperboloid gear is created by revolving the gear profile, offsetting the result to create wall thickness and then gouging out the grooves. In practice however, the third step is significantly more complex as it involves creating spirals, with a rectangular cross-section whose rectangular faces are constantly normal to the doubly curved surface which it follows. To make matters worse, the two curvatures, as well as the spiral properties and groove depth/width could change on any given design iteration. The way this sub-stage functions can be explained in five steps (figure 3.8):

First the gear profile is revolved to generate the outer surface of the finished

mechanism. Along with it, is generated an annulus whose radius is the arc length of the gear profile and whose inner diameter matches the smallest of the mechanisms surface two diameters. This serves to create a flat approximations of the revolved profile. From there a spiral is drawn on the annulus with the desired number of turns (calculated from the desired opening rate). By using UV mapping from the annulus onto the revolved surface, the spiral can be mapped onto the mechanism shape while preserving an approximate constant distance along the surface between each turn. The spiral on the revolved surface can then be offset within that surface to the required groove width, drawing the outline of the groove. Having done this, it is possible to subdivide the two curves into a large number of points. Each of those points being on the revolved surface, it is possible to calculate the surface normal at each of the points before offsetting them normal to the surface by the required groove depth. These new points which are now offset from the surface can then be interpolated into a new curve which, when paired with the one on the original surface, can be made to form the ”negative” of the groove. At this point the revolved surface is also offset by a value slightly greater than the groove depth to give it a thickness. The last step consists in subtracting the groove negative from the thickened revolution of the gear profile.

Though the refinement phase performs other smaller housekeeping operations, these three are good examples of how the models loose ends can be tied together by careful analysis of the process and results. They also show how much these operations are guided by experience and are thus subjective design decisions.

3.2.5 Export

The last phase as defined in the introduction is the export phase. Each part of the platforms 3D printed structure is conceptualized with a certain 3D printed orientation in mind: for example, the structure section are cut flat for better adhesion and the arms

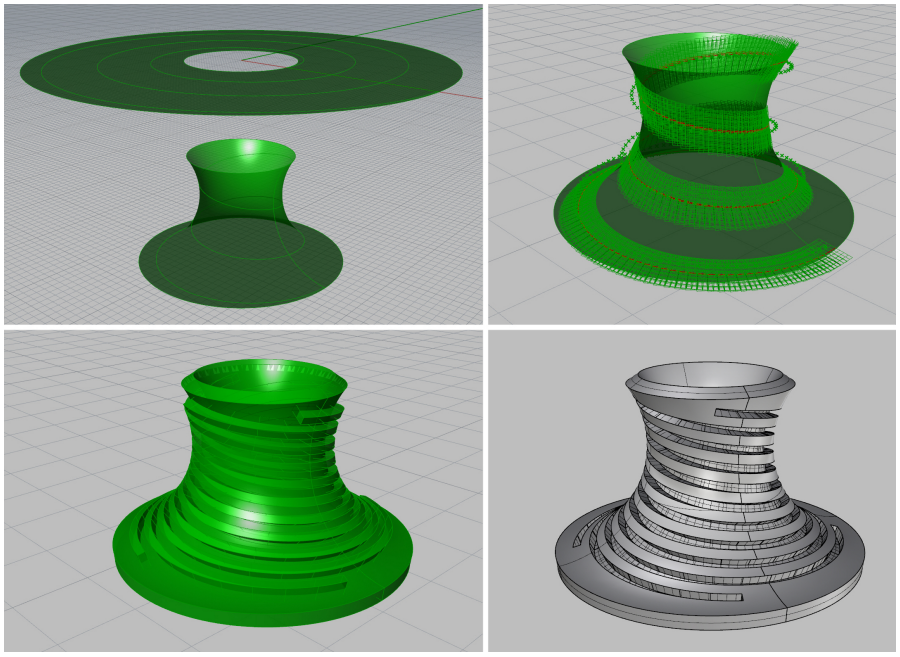

Figure 3.8: Intermediary steps in the creation of the hyperboloid model.

are extruded and printed on their side to ensure the printing layers are aligned with main stresses expected in the arm. For this reason, the optimization process does very little analysis, only rotating pre-specified components in pre-specified way before exporting them to pre-specified files.

Chapter 4

Conclusion

The goal of this thesis being to explore the development of a 3D printed, GLAD platform for on-site exploration by using a multi-disciplinary optimization process to allow for the creation of adaptive designs of shape-changing UAVs, thus the success of endeavor can be defined in two parts. The first measure of success which was attained is the demonstration of conceptual validation of the a 3D printed GLAD platform. Through the use of FEA analyses, physical tests and prototypes, it was demonstrated that it is indeed possible to create 3D printed structure capable of theoretically withstanding launch loads in excess of 10Gs and deploying autonomously, while remaining light, streamlined and versatile. With this said further physical testing is required to properly assess the various component's capacity to withstand these forces as a system, including mechanical connections and electronic components. The second goal of this thesis being to explore the development of a multi-disciplinary optimization process to allow for the adaptive designs of these platforms, its' success can be assessed by looking at the final outputs it was able to generate. To do this, three different outputs, stemming from different input configurations are studied. The three batches of input are chosen pseudo-randomly to reflect possible design requirement. The first aims for a small form, short endurance

platform by the use of smaller propellers, quad layout, no payload, small PCB, short stepper motor and a tight maximum barrel diameter. The second aims for a more standard hexacopter platform with mid-range components. Lastly, the last design set forth in this comparison uses larger components from the PCB, to the motors and propellers with a very large maximum diameter allowed. For each of these, the results are presented in figure 4.1, showing the layout chosen, shell shape, as well as the fully generated mechanism and arm structure.

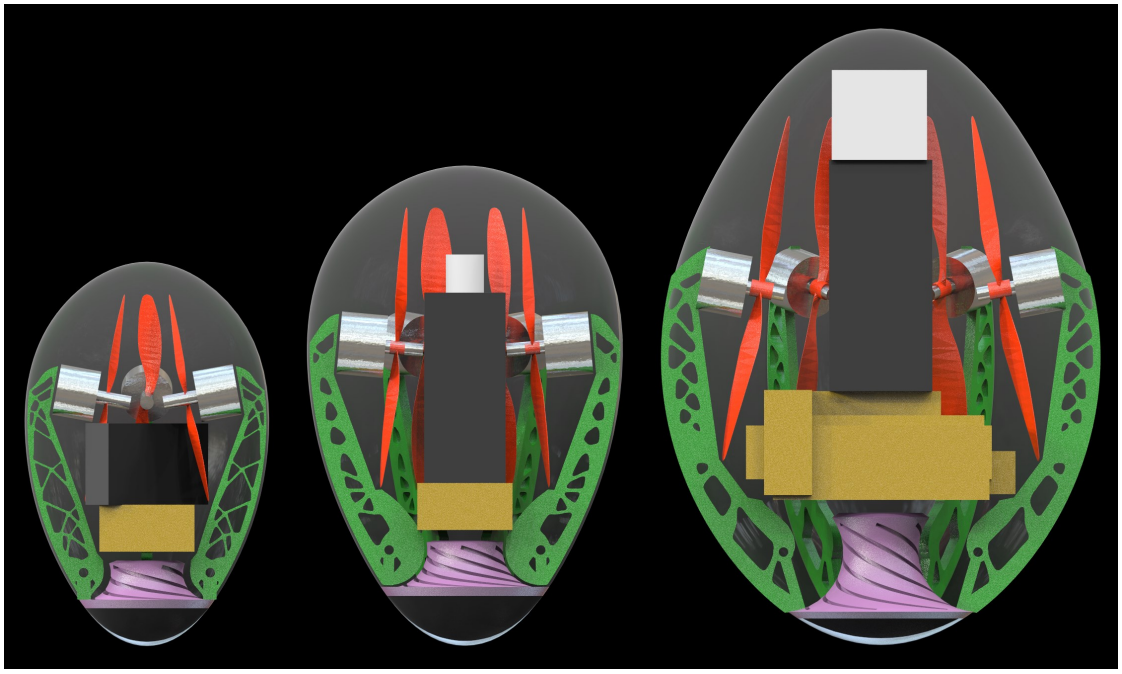

Figure 4.1: Three different designs outputted by the optimization process, respectively optimized (from left to right) for small size, standard operations or long endurance.

These examples illustrate the great flexibility demonstrated by the optimization process, allowing it to generate the following designs given a wide range of inputs. One notable item missing from these results is the main body's structure whose design's computational weight remains one of the largest impediments to the full implementation of this optimization process. At this point, the structure for any design must still be hand-drafted based loosely on the coarse output of the 3D topology optimization.

Despite this missing step in the process, GLAD design were successfully produced and built through this optimization process, such as the one presented below. This particular model was optimized to fit inside a 6 inch diameter sphere. Additionally, it can be compared next to the original GLAD platform before optimization thus highlighting how the design process, using the same components as the original platform, created a more functional, smaller design (figure 4.2).

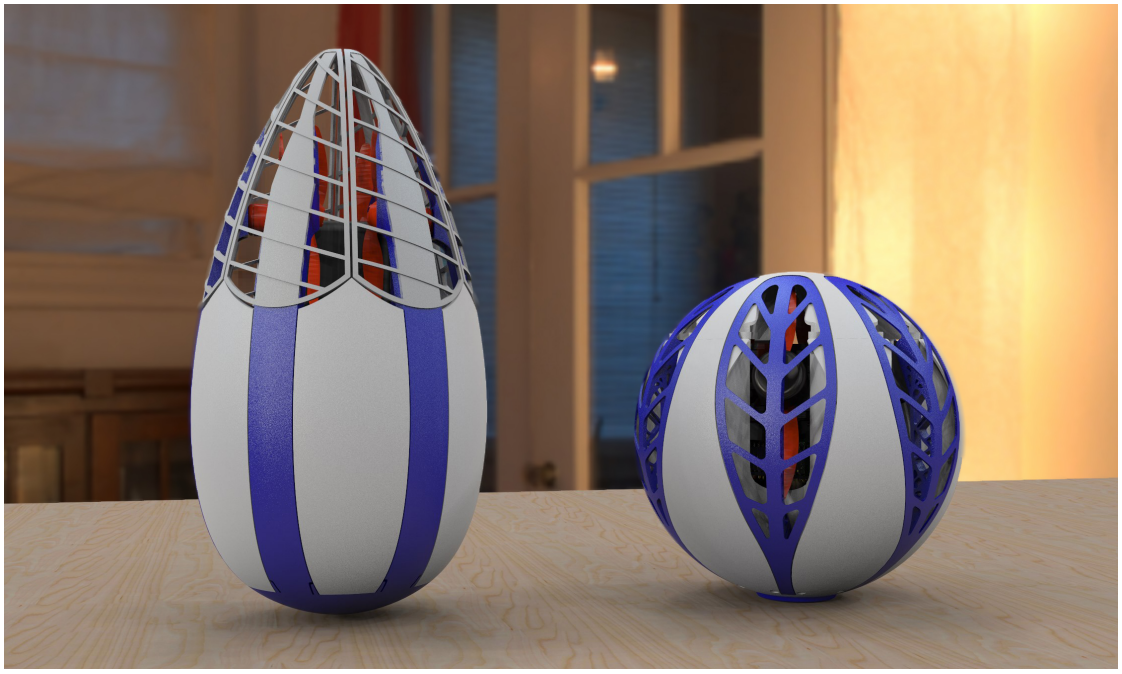

Figure 4.2: Original GLAD platform design compared to the functional design created by inputting the same electro-mechanical components into the adaptive design model.

Overall, the optimization process succeeded in the creation of designs, but many areas still need to be ironed out to ensure smooth functioning in all conditions, the creation of the shell's structure and user-friendliness of the design experience. It is also interesting to note that, if further implemented, many of the design decisions could be better served through the use of machine learning techniques instead of empirical, conditional processes.

Bibliography

[1] Richter, A. M., Petrovic, V., Kuester, F., Seracini, M., and Angelo, R., "From STEM to STEAM: Towards aerospace partnerships with cultural heritage diagnostics." *IEEE Aerospace Conference*, 2014, pp. 1–11.

[2] Olsen, M. J., Kuester, F., Chang, B. J., and Hutchinson, T. C., "Terrestrial laser scanning-based structural damage assessment." *JComputing in Civil Engineering*, Vol. 24.3, 2010, pp. 264–272.

[3] Tulldahl, M. H. and Larsson, H., "Lidar on small UAV for 3D mapping." *Proc. SPIE*, Vol. 9250, 2014, pp. 925009–925009–14.

[4] Suárez, J. C., Ontiveros, C., Smith, S., and Snape, S., "Use of airborne LiDAR and aerial photography in the estimation of individual tree heights in forestry," *Computers & Geosciences*, Vol. 31, No. 2, 2005, pp. 253–262.

[5] Gnemmi, P., Changey, S., Meder, K., Roussel, E., Rey, C., Steinbach, C., and Berner, C., "Conception and Manufacturing of a Projectile-Drone Hybrid System," *IEEE/ASME Transactions on Mechatronics*, Vol. 22, No. 2, April 2017, pp. 940–951.

[6] Hargroves, K. and Smith, M., "Innovation inspired by nature: biomimicry," *Ecos*, Vol. 2006, No. 129, 2006, pp. 27–29.

[7] Berman, B., "3-D printing: The new industrial revolution," *Business horizons*, Vol. 55, No. 2, 2012, pp. 155–162.

[8] Rechenberg, I., "The Evolution Strategy. A Mathematical Model of Darwinian Evolution," *Synergetics From Microscopic to Macroscopic Order*, Vol. 22, pp. 122–132.

[9] Rechenberg, I., "Case studies in evolutionary experimentation and computation," *Computer Methods in Applied Mechanics and Engineering*, Vol. 186, No. 2–4, 2000, pp. 125–140.

[10] Vecchi, S. K. C. D. G. M. P., "Optimization by Simulated Annealing," *Science*, Vol. 220, 1983, pp. 671–680.

[11] Remouchamps, A., Bruyneel, M., Fleury, C., and Grihon, S., "Application of a bi-level scheme including topology optimization to the design of an aircraft pylon," *Structural and Multidisciplinary Optimization*, Vol. 44, No. 6, 2011, pp. 739–750.

[12] Grihon, S., Krog, L., and Bassir, D., "Numerical Optimization applied to structure sizing at AIRBUS: A multi-step process," *International Journal for Simulation and Multidisciplinary Design Optimization*, Vol. 3, No. 4, 2009, pp. 432–442.

[13] D. Brackett, I. Ashcroft, R. H., "TOPOLOGY OPTIMIZATION FOR ADDITIVE MANUFACTURING," 2011.

[14] Ferro, C., Grassi, R., Secli, C., and Maggiore, P., "Additive Manufacturing Offers New Opportunities in UAV Research," *Procedia CIRP*, Vol. 41, 2016, pp. 1004–1010.

[15] Zhu, J.-H., Zhang, W.-H., and Xia, L., "Topology Optimization in Aircraft and Aerospace Structures Design," *Archives of Computational Methods in Engineering*, Vol. 23, No. 4, 2016, pp. 595–622.

[16] Gerhard, V. and Sobieszczanski-Sobieski, J., "Multidisciplinary Optimization of a Transport Aircraft Wing using Particle Swarm Optimization," *9th AIAA/ISSMO Symposium on Multidisciplinary Analysis and Optimization*, 2002.

[17] Cheng, S.-W., "Rapid Deployment UAV," 2008, pp. 1–8.

[18] Bendea, H., Boccardo, P., Dequal, S., Giulio Tonolo, F., Marenchino, D., and Piras, M., "Low cost UAV for post-disaster assessment," *The International Archives of the Photogrammetry, Remote Sensing and Spatial Information Sciences*, Vol. 37, No. Part B, 2008, pp. 1373–1379.

[19] Ochi, S., "Development of high strength biodegradable composites using Manila hemp fiber and starch-based biodegradable resin," *Composites part A: Applied science and manufacturing*, Vol. 37, No. 11, 2006, pp. 1879–1883.

[20] Koh, L. and Wich, S., "Dawn of drone ecology: low-cost autonomous aerial vehicles for conservation." *Tropical Conservation Science*, 2012, pp. 121–132.

[21] Dumont, J. N. and Brummett, A. R., "Egg envelopes in vertebrates," 1985, pp. 235–288.

[22] Mungan, C. E., "Internal ballistics of a pneumatic potato cannon," *European Journal of Physics*, Vol. 30, No. 3, 2009, pp. 453.

[23] Holtzman, A. L. and Goodson, F. R., "Plastic composite sabot," April 5 1988, US Patent 4,735,148.

[24] Tymrak, B., Kreiger, M., and Pearce, J., "Mechanical properties of components fabricated with open-source 3-D printers under realistic environmental conditions," *Materials & Design*, Vol. 58, 2014, pp. 242 – 246.

[25] Henderson, L. W., Glaser, T. C., and Kuester, F., "Towards Bio-Inspired Structural Design of a 3D Printable, Ballistically Deployable, Multi-Rotor UAV," *IEEE Aerospace Conference*, 2017, pp. 1–7.